

A
Project report
on
CFD simulation of Bed expansion and Gas hold up behaviour of Gas-Liquid-Solid Fluidized Bed

Submitted by
LIPIKA KALO
Roll No. 210CH1263

In partial fulfillment of
Master of Technology (Chemical Engg.)

Under the Guidance of
DR. H.M. JENA



Department of Chemical Engineering
National Institute of Technology
Rourkela
2012

**National Institute of Technology
Rourkela**



CERTIFICATE

This is to certify that the seminar report entitled, “CFD Simulation of Bed expansion and Gas hold up behaviour of Gas-Liquid-Solid Fluidized Bed” submitted by Lipika Kalo (Roll No-210CH1263) in partial fulfilment of the requirements of the degree of Master of Technology in Chemical Engineering at National Institute of Technology, Rourkela is prepared by her under my supervision and guidance.

Date:

DR. H. M. JENA
Dept. of Chemical Engineering
National Institute of Technology

ACKNOWLEDGEMENT

I take this opportunity to express my sense of gratitude and indebtedness to Dr. H.M. Jena, Department of Chemical Engineering for helping me a lot to complete the seminar work without whose sincere and kind effort, this seminar would not have been success.

Date:

Lipika Kalo

Roll. No.: 210CH1263

4th Semester, M. Tech

Chemical Engineering

CONTENTS

| | |
|---|-----------|
| COVER PAGE | i |
| CERTIFICATE | ii |
| ACKNOWLEDGEMENT | iii |
| CONTENTS | iv |
| ABSTRACT | vi |
| LIST OF FIGURES | vii |
| LIST OF TABLES | ix |
| NOMENCLATURE | x |
| 1.0 INTRODUCTION | 1 |
| 1.1 Three phase fluidized bed | 1 |
| 1.2 Advantages of Three-phase Fluidized Beds | 2 |
| 1.3 Application of Three phase fluidized bed | 3 |
| 1.4 Drawbacks of Fluidized bed | 3 |
| 1.5 Modes of operation of Gas-Liquid-Solid Fluidized bed and Flow Regimes | 4 |
| 1.6 Variables affect the quality of Fluidization | 5 |
| 1.7 Complexion of Three phase system | 6 |
| 1.8 Present work | 6 |
| 1.9 Thesis Layout | 7 |
| 2.0 LITERATURE REVIEW | 12 |
| 3.0 CFD MODELLING OF THREE PHASE FLUIDIZED BED | 12 |
| 3.1 CFD (Computational Fluid Dynamics) | 12 |
| 3.2 Advantages of CFD | 13 |
| 3.3 Limitations of CFD | |

| | |
|--|-----------|
| 3.4 Applications of CFD | 13 |
| 3.5 Working of CFD | 14 |
| 3.6 Discretization Methods in CFD | 16 |
| 3.7 Approaches to Multiphase modelling | 18 |
| 3.8Computational Flow model | 21 |
| 3.9Numerical Methodology | 22 |
| 3.10 Phase Dynamics | 25 |
| 3.11 Gas hold up | 26 |
| 3.12 Bed Expansion | 37 |
| 4.0 CONCLUSION | 39 |
| REFERENCES | 40 |

Abstract

Three-phase fluidization is a process used to bring into contact gas, liquid and solids, and in which the solid particles are kept in suspension by a through flow of liquid. Three-phase fluidized beds are used extensively in the refining, petrochemical, pharmaceutical, biotechnology, food and environmental industries. The fundamental characteristics of a three-phase fluidized bed have been recently studied extensively. The gas holdup is one of the most important characteristics for analysing the performance of a three-phase fluidized bed. In the present work FLUENT has been used to study gas-liquid-solid fluidization. CFD simulations have been done for a column of height 1.88 m and diameter 0.1 m containing glass beads as solid particles of size 2.18 mm. In the present work, involving three phase fluidized bed, CFD analysis of gas holdup and bed expansion behaviour have been studied. ANSYS has been used to generate a 3D fine grid. The gas (air) and liquid (water) is injected at the base with different velocities.

LIST OF FIGURES

| FIGURE NO. | DESCRIPTION | PAGE NO. |
|------------|--|----------|
| 3.1 | 3D mesh | 23 |
| 3.2 | Contours of volume fraction of air at water velocity of 0.12 m/s and air velocity of 0.025m/s for initial bed height of 21.3 cm. | 25 |
| 3.3 | Contours of volume fraction of solid, liquid and gas at water velocity of 0.12 m/s and air velocity of 0.025 m/s for initial static bed height of 0.213 m. | 26 |
| 3.4 | Variation of gas holdup with liquid velocity at constant air velocity for 2.18 mm glass beads at $H_s = 0.213$ m. | 27 |
| 3.5 | comparison of the gas holdup of air velocity 0.0625 m/s | 28 |
| 3.6 | Variation of gas holdup with gas velocity at constant liquid velocity for 2.18 mm glass beads at $H_s = 0.213$ m. | 28 |
| 3.7 | Volume fraction of air along axial direction in 1.88 m fluidized bed at [$V_l = 0.12$ m/s, $V_g = 0.0375$ m/s, $H_s = 0.213$ m, $D_p = 2.18$ mm] on x-x' axis | 29 |
| 3.8 | Volume fraction of solid along axial direction in 1.88 m fluidized bed at [$V_l = 0.12$ m/s, $V_g = 0.0375$ m/s, $H_s = 0.213$ m, $D_p = 2.18$ mm] on x-x' axis | 30 |

| | | |
|------|--|----|
| 3.9 | Volume fraction of liquid along axial direction in 1.88 m fluidized bed at [$V_l=0.12$ m/s, $V_g=0.0375$ m/s, $H_s=0.213$ m, $D_p=2.18$ mm] on x-x' axis | 30 |
| 3.10 | Volume fraction of air along axial direction in 1.88 m fluidized bed at [$V_l=0.12$ m/s, $V_g=0.0375$ m/s, $H_s=0.213$ m, $D_p=2.18$ mm] on y-y' axis | 31 |
| 3.11 | Volume fraction of solid along axial direction in 1.88 m fluidized bed at [$V_l=0.12$ m/s, $V_g=0.0375$ m/s, $H_s=0.213$ m, $D_p=2.18$ mm] on y-y' axis | 32 |
| 3.12 | Volume fraction of liquid along axial direction in 1.88 m fluidized bed at [$V_l=0.12$ m/s, $V_g=0.0375$ m/s, $H_s=0.213$ m, $D_p=2.18$ mm] on y-y' axis | 32 |
| 3.13 | Volume fraction of air with different bed height along radial direction in 1.88 m fluidized bed at [$V_l=0.12$ m/s, $V_g=0.0375$ m/s, $H_s=0.213$ m, $D_p=2.18$ mm] on x-x' axis | 33 |
| 3.14 | Volume fraction of glass bead with different bed height along radial direction in 1.88 m fluidized bed at [$V_l=0.12$ m/s, $V_g=0.0375$ m/s, $H_s=0.213$ m, $D_p=2.18$ mm] on x-x' axis | 34 |
| 3.15 | Volume fraction of water with different bed height along radial direction in 1.88 m fluidized bed at [$V_l=0.12$ m/s, | 34 |

| | | |
|------|---|----|
| | $V_g=0.0375$ m/s, $H_s=0.213$ m, $D_p=2.18$ mm] on x-x' axis | |
| 3.16 | Volume fraction of air with different bed height along radial direction in 1.88 m fluidized bed at [$V_l=0.12$ m/s, $V_g=0.0375$ m/s, $H_s=0.213$ m, $D_p=2.18$ mm] on y-y' axis | 35 |
| 3.17 | Volume fraction of solid with different bed height along radial direction in 1.88 m fluidized bed at [$V_l=0.12$ m/s, $V_g=0.0375$ m/s, $H_s=0.213$ m, $D_p=2.18$ mm] on y-y' axis | 36 |
| 3.18 | Volume fraction of water with different bed height along radial direction in 1.88 m fluidized bed at [$V_l=0.12$ m/s, $V_g=0.0375$ m/s, $H_s=0.213$ m, $D_p=2.18$ mm] on y-y' axis | 36 |
| 3.19 | Variation of bed height with gas velocity for 2.18 mm glass beads at $H_s= 0.213$ m. | 37 |
| 3.20 | Variation of bed height with liquid velocity for 2.18 mm glass beads at $H_s= 0.213$ m | 38 |

LIST OF TABLES

| Table No. | Topic | Page |
|-----------|----------------------------------|------|
| 3.1 | Mesh Information | 23 |
| 3.2 | Value of various model constants | 23 |

NOMENCLATURE

| | |
|-----------------|--|
| ρ_k | density of phase k = gas, liquid, solid, kg m^{-3} |
| ε_k | volume fraction of phase k = gas, liquid, solid, - |
| u_k | velocity of phase k = gas, liquid, solid, m/s |
| ∇p | pressure drop in gas-liquid-solid fluidized bed, Pa |
| τ_k | stress-strain tensors of phase k = gas, liquid, solid, Pa |
| g | acceleration due to the gravity, ms^{-2} |
| $F_{i,k}$ | inter-phase momentum exchange coefficient for phase k , $\text{kg}/(\text{m}^3 \text{ s})$ |
| K_{Ls} | inter-phase exchange coefficient between liquid and solid phases, kgs^{-1} |
| μ_L | liquid viscosity, Pa s |
| ρ_L | density of liquid, kg m^{-3} |
| d_p | average particle diameter, m |
| Re_p | particle Reynolds number, - |
| Re_b | bubble Reynolds number, - |
| C_D | Drag co-efficient, - |

Subscripts

| | |
|-----|--------------|
| g | gas phase |
| l | liquid phase |
| s | solid phase |

CHAPTER-1

1.0 Introduction

Fluidization is an operation through which fine solids are transformed into a fluid like state through contact with either a gas, liquid or both. Under the fluidized state, the gravitational pull on granular solid particles is offset by the fluid drag on them, thus the particles remain in a semi-suspended condition. At the critical value of fluid velocity the upward drag forces exerted by the fluid on the solid particles become exactly equal the downward gravitational forces, causing the particles to become suspended within the fluid. At this critical value, the bed is said to be fluidized and exhibit fluidic behavior.

1.1 Three phase fluidized bed

The three phase fluidized bed is a type of system that can be used to carry out a variety of multiphase chemical reactions. In this type of reactor, gas and liquid are passed through a granular solid material at high enough velocities to suspend the solid in fluidized state. The solid particles in the fluidized bed are typically supported by a porous plate, known as a distributor at the static condition. The fluid is then forced through the distributor up through the solid material.

At lower fluid velocities, the solids remain in place as the fluid passes through the voids in the material. As the fluid velocity is increased, the bed reaches a stage where the force of the fluid on the solids is enough to balance the weight of the solid material. This stage is known as incipient fluidization and the corresponding fluid velocity is called the minimum fluidization velocity. Once this minimum velocity is surpassed, the contents of the bed begin to expand and swirl around much like an agitated tank or boiling pot of water, the system is now a fluidized bed. Three-phase fluidized bed reactors are used extensively in chemical, petrochemical, refining, pharmaceutical, biotechnology, food and environmental industries. The most common occurrence of gas-liquid-solid phase systems is in hydro processing industry in which variety of reactions between hydrogen and oil phase with solid catalyst have been found. The other common three phase reactions are catalytic oxidation and hydration reactions. Three phase fluidization systems, the phase are reacting with different forms as:

- Reactions where the gas, liquid and solid are either reactants or products.

- Gas-Liquid reactions with solid as a catalyst.
- Two reaction phases and third as inert phase.
- All three phases are inert as found in unit operations.

Depending on the density and volume fraction of particles, three-phase reactors can be classified as slurry bubble column reactors and fluidized bed reactors. In slurry bubble column reactors, the density of the particles are slightly higher than the liquid and particle size is in the range of 5-150 μm and volume fraction of particles is below 0.15 hence, the liquid phase along with particles is treated as a homogenous liquid with mixture density. But in fluidized bed reactors, the density of particles are much higher than the density of the liquid and particle size is normally large (above 150 μm) and volume fraction of particles varies from 0.6 (packed stage) to 0.2 as close to dilute transport stage (Panneerselvam et al., 2009).

Various hydrodynamic characteristics of three-phase fluidized beds such as hold up of all three phases, bed expansion, pressure drop, velocity profile have been studied. The hydrodynamic characteristic gas holdup is one of the most important characteristic for analyzing the performance of three-phase fluidized bed. For chemical processes, where mass transfer is the rate-limiting step, it is important to estimate the gas holdup since this relates directly to the rate of mass transfer. It measures the fractional volume occupied by the gas. Bed expansion is also one of the important factors which is considered in the design of fluidized beds. It gives the height of fluidized bed during operation.

1.2 Advantages of three phase fluidized bed

The three phase fluidized beds are increasingly used as reactors as they overcome some inherent drawback of conventional reactors and add more advantages. Some of the advantages of three phase fluidized bed reactor are as follow (Trambouze and Euzen., 2004). High rate of reaction per unit reactor volume can be obtained through these reactors. The major advantages of these reactors are, they give high turbulence, better flexibility of mixing, heat recovery and temperature control. The better mixing and in these reactors prevents the formation of local hot spots. The three phase fluidized bed offers better gas phase distribution creating more gas-liquid interfacial area. Ability to continuously withdraw product and introduce new reactants into the reaction vessel allows production more efficiently due to the removal of startup conditions as in case of batch processes. They allow use of fine catalyst particles, which minimizes the intra

particle diffusion. Smaller is the particle larger is surface area which enables more intimate contact of phases and enhances the reactor performance. These reactors can effectively be used for the rapidly deactivating catalyst and three phase reactions where solid is catalyst and also solid is used as reactant (e.g. catalytic coal liquefaction). Bubbling and circulating fluidized bed systems are becoming an increasingly important in technology for the power generation, mineral and chemical processing industries. Benefits in economic, operational and environmental terms can be achieved with fluidized bed technology over more traditional technologies.

1.3 Application of Three phase fluidized bed

The gas-liquid-solid fluidized bed has emerged in recent years as one of the most promising devices for three-phase operation. Such a device is of considerable industrial importance as evident from its wide application in chemical, petrochemical and biochemical processing (Muroyama et al., 1985). Fluidized beds serve many purposes in industry, such as facilitating catalytic and non-catalytic reactions. Three-phase fluidized beds have been applied successfully to many industrial processes such as in the Hydrogen-oil process for hydrogenation and hydro-desulfurization of residual oil, the H-coal process for coal liquefaction and Fischer-Tropsch process (Jena et al., 2009). Some more applications of fluidized bed are:

- Turbulent contacting absorption for flue gas desulphurization.
- Bio-oxidation process for waste water treatment.
- Physical operations such as drying and other forms of mass transfer.
- Biotechnological processes such as fermentation and aerobic waste water treatment.
- Methanol production and conversion of glucose to ethanol.
- Pharmaceuticals and mineral industries.
- Oxidation of naphthalene to phthalic anhydride (catalytic).
- Coking of petroleum residues (non-catalytic).

1.4 Drawbacks of fluidized bed

As in any design, the fluidized bed reactor does have its draw-backs, which any reactor designer must take into consideration (Trambouze and Euzen, 2004).

Increased Vessel Size: Because of the expansion of the bed materials in the reactor, a larger vessel is often required than that for a packed bed reactor. This larger vessel means that more must be spent on initial capital costs.

Pumping Requirements and Pressure Drop: The requirement for the fluid to suspend the solid material necessitates that a higher fluid velocity is attained in the reactor. In order to achieve this, more pumping power and thus higher energy costs are needed. In addition, the pressure drop associated with deep beds also requires additional pumping power.

Particle Entrainment: The high gas velocities present in this reactor often result in fine particles becoming entrained in the fluid. These captured particles are then carried out of the reactor with the fluid, where they must be separated. This can be a very difficult and expensive problem to address depending on the design and function of the reactor.

Erosion of Internal Components: The fluid-like behavior of the fine solid particles within the bed eventually results in the wear of the reactor vessel. This can require expensive maintenance and upkeep for the reaction vessel and pipes.

Lack of Current Understanding: Current understanding of the actual behavior of the materials in a fluidized bed is rather limited. It is very difficult to predict and calculate the complex mass and heat flows within the bed. Due to this lack of understanding, a pilot plant for new processes is required. Even with pilot plants, the scale-up can be very difficult and may not reflect what was experienced in the pilot trial.

1.5 Modes of operation of gas-liquid-solid fluidized bed

Gas-liquid-solid fluidization can be classified mainly into four modes of operation. These modes are:

- Co-current three phase fluidization with liquid as the continuous phase.
- Co-current three phase fluidization with gas as the continuous phase.
- Inverse three phase fluidization.
- Fluidization by a turbulent contact absorber.

Based on the differences in flow directions of gas and liquid and in contacting patterns between the particles and the surrounding gas and liquid, several types of operation for gas-liquid-solid fluidizations are possible. Three-phase fluidization is divided into two types according to the relative direction of the gas and liquid flows, namely, co-current three-phase fluidization and counter-current three-phase fluidization (Bhatia and Epstein, 1974b; Epstein, 1981).

1.6 Variables affecting the quality of fluidization

Some of the variables affecting the quality of fluidization are as follow:

Fluid flow rate: It should be high enough to keep the solids in suspension but it should not be so high that the fluid channeling occurs.

Fluid inlet: It must be designed in such a way that the fluid entering the bed is well distributed.

Bed height: With other variables remaining constant, the greater the bed height, the more difficult it is to obtain good fluidization.

Particle size: It is easier to maintain fluidization quality with particles having a wide range than with particles of uniform size.

Gas, Liquid and solid densities: The closer the relative density of the gas, liquid and the solid, the easier is to maintain smooth fluidization.

1.7 Complexion of three phase system

Selection and design of reactors is one of the main parameter in the performance of three phase system. As three-phase system is highly complex and the success of three-phase system is essentially dependent on the effective contact of each phase with other. Even though a large number of experimental studies have been carried out for different process parameters and physical properties, the complex hydrodynamics of three-phase fluidized bed reactors are not well understood due to complicated phenomena such as particle-particle, liquid-particle and particle-bubble interactions. For this reason, computational fluid dynamics (CFD) has been promoted as a useful tool for understanding multiphase reactors (dudukovic et al., 1999) for precise design and scale up. By using CFD various reactors and phase contactors were studied and operated successfully.

1.8 Present work

The present work is concentrated on understanding the complex hydrodynamics of three-phase fluidized beds. Fluidized bed of height 1.88 m and diameter 0.1 m have been simulated. The solid phase used is glass beads of size 2.18 mm in the present work. Co-current gas-liquid-solid fluidization with liquid as continuous phase has been used. The static bed heights of the solid phase in the fluidized bed used for simulation are taken as 21.3 cm. Initial solid hold up has been taken as 0.59 in all cases with superficial velocity of gas varying in the range of 0.025-0.1 m/sec and that of the liquid ranges to 0.02-0.16 m/s.

The CFD simulations have been carried out using commercial CFD software ANSYS FLUENT 13. The aim is to simulate the three phase fluidized bed to find out the effect of various operating parameters on the hydrodynamics. The hydrodynamics parameters for investigation are bed expansion and gas hold up.

1.9 Thesis layout

The second chapter of thesis contains a detailed literature survey of computational work on three phase fluidization. The detail description of CFD modeling of three phase fluidized bed, detail descriptions of numerical techniques and methods for solving computational model and various approaches applied in CFD modeling have been discussed in third chapter. The results obtained from CFD simulation have been presented and discussed. In the last chapter conclusion have been drawn on present work.

CHAPTER 2

2.0 Literature Review

A significant amount of experimental study on the hydrodynamic and other characteristic behavior of three phase fluidized bed has been carried out. Most of the previous studies related to three-phase fluidized bed reactors have been directed towards the understanding the complex hydrodynamics, and its influence on the phase holdup and transport properties. Recent research on fluidized bed reactors focuses on flow structure and flow regime identification is being discussed below:

Flow structure quantification: The quantification of flow structure in three-phase fluidized beds mainly focuses on local and globally averaged phase holdups and phase velocities for different operating conditions and parameters. Rigby et al. (1970), Muroyama and Fan (1985), Lee and De Lasa (1987) investigated bubble phase holdup and velocity in three-phase fluidized beds for various operating conditions using experimental techniques like electro resistivity probe and optical fiber probe. Recently Warsito and Fan (2001, 2003) quantified the solid and gas holdup in three-phase fluidized bed using the electron capacitance tomography (ECT) (Panneerselvam, 2009).

Flow regime identification: Muroyama and Fan (1985) developed the flow regime diagram for air-water-particle fluidized bed for a range of gas and liquid superficial velocities. Chen et al. (1995) investigated the identification of flow regimes by using pressure fluctuations measurements. Briens and Ellis (2005) used spectral analysis of the pressure fluctuation for identifying the flow regime transition from dispersed to coalesced bubbling flow regime based on various data mining methods like fractal and chaos analysis, discrete wake decomposition method etc. Fraguío et al. (2006) used solid phase tracer experiments for flow regime identification in three-phase fluidized beds (Panneerselvam, 2009).

Some of the various investigations done by researchers on three phase fluidization are mentioned below:

- Kiared et al. (1999) have investigated the solid phase hydrodynamics in three-phase fluidized bed using radioactive particle tracking. Experimental descriptions of the time-averaged solids flow in the fully developed region of a cylindrical gas-liquid-solid fluidized bed have been provided by using a non-invasive radioactive particle tracking

technique (RPT). The 3-D local instantaneous velocity components (radial, axial, azimuthal) of a single radioactive solid tracer have been measured over extended time period. Radial distributions of axial and radial mean turbulent velocities of particle, shear stress and eddy diffusion coefficients have been established.

- Sokol and Halfani (1999) have studied the hydrodynamics of gas-liquid-solid fluidized bed bioreactor with a low density biomass support (matrix density smaller than that of water). It has been found that the air holdup increases with increase in the inlet air velocity.
- Allia et al. (2006) have carried out the hydrodynamic study of three phase fluidized bed bioreactors used for the removal of hydrocarbons from the refinery waste water. The study allowed the determination of operating conditions before treatment experiments. The obtained results have shown that in the three-phase fluidized bed the hydrocarbons degrade more rapidly than in a closed aerated bioreactor.

Even though a large number of experimental studies have been directed towards the quantification of flow structure and flow regime identification for different process parameters and physical properties, the complex hydrodynamics of these reactors are not well understood due to the interaction of all the three phases simultaneously. It has been a very tedious task to analyze the hydrodynamic property in experimental way of three phase fluidized bed reactor, so another advanced modeling approaches based on CFD techniques have been applied for investigation of three phases for accurate design and scale up. Basically two approaches namely, the Euler-Euler formulation based on the interpenetrating multi-fluid model, and the Euler-Lagrangian approach based on solving Newton's equation of motion for the dispersed phase are used.

2.2 Survey on CFD modeling

- Bahary et al. (1994) have used Eulerian multi-fluid approach for three-phase fluidized bed, where gas phase treated as a particulate phase having 4 mm diameter and a kinetic theory granular flow model applied for solid phase. They have simulated both symmetric and axisymmetric model and verified the different flow regimes in the fluidized bed by comparing with experimental data.
- Grevschott et al. (1996) have used Eulerian-Eulerian model approaches for three-phase bubble column. The liquid phase along with the particles has been considered pseudo-

homogeneous by modifying the viscosity and density. The bubble size distribution based on the bubble induced turbulent length and the local turbulent kinetic energy has been studied. Variations of bubble size distribution, liquid circulation and solid movement along radial direction have been discussed.

- Mitra-Majumdar et al. (1997) have taken multi-fluid Eulerian approach for three-phase bubble column. They have used modified drag correlation between the liquid and the gas phase to account for the effect of solid particles and between the solid and the liquid phase to account for the effect of gas bubbles. A $k-\epsilon$ turbulence model has been used for the turbulence and considered the effect of bubbles on liquid phase turbulence. Axial variation of gas holdup and solid holdup profiles for various range of liquid and gas superficial velocities and solid circulation velocity have been examined.
- Jianping and Shonglin (1998) have worked in 2-D with Eulerian-Eulerian method for $k-e-k-e$ three-phase bubble column for turbulence. Turbulence model and Pseudo-two-phase fluid dynamic model have been used. The local axial liquid velocity and local gas holdup with have been validated experimental data.
- Li et al. (1999) have studied in 2-D with Eulerian-Lagrangian model for three-phase fluidization. The Eulerian fluid dynamic method, the dispersed particle method (DPM) and the volume-of-fluid (VOF) method have been used to account for the flow of liquid, solid and gas phases respectively. A continuum surface force (CSF) model, a surface tension force model and Newton's third law have been applied to account for the interphase couplings of gas-liquid, particle-bubble and particle-liquid interactions respectively. A close distance interaction (CDI) model included in the particle-particle collision analysis, which considers the liquid interstitial effects between colliding particles. Single bubble rising velocity in a liquid-solid fluidized bed and the bubble wake structure and bubble rise velocity in liquid and liquid-solid medium have been investigated.
- Padial et al. (2000) have worked in 3-D with multi-fluid Eulerian approach for three-phase draft-tube bubble column. The drag force between solid particles and gas bubbles has been modeled in the same way as that of drag force between liquid and gas bubbles. The gas volume fraction and liquid circulation in draft tube bubble column have been simulated.

- Joshi et al. (2001) have studied the bubble column reactors using Computational flow modeling with Euler-Lagrange approach. Understanding of the drag force, virtual mass force and lift force and mechanism of the energy transfer from gas to liquid phase have been explained. By using phases flow pattern results the effort has been concentrated to design cylindrical bubble column. The effects of the superficial gas velocity, column diameter and bubble slip velocity on the flow pattern have been examined and compared with experimental velocity profiles.
- Matonis et al. (2002) have worked in 3-D with multi-fluid Eulerian approach for slurry bubble column and used the Kinetic theory granular flow (KTGF) model for describing the particulate phase. The $k-\epsilon$ based turbulence model has been taken for liquid phase turbulence and the analysis of the time averaged solid velocity, volume fraction profiles, shear Reynolds stress have been done and compared with experimental data.
- Feng et al. (2005) have used 3-D, multi-fluid Eulerian approach for three-phase bubble column. The liquid phase along with the solid phase considered as a pseudo-homogeneous phase in view of the ultrafine nanoparticles. The interface force model of drag, lift and virtual mass and $k-\epsilon$ model for turbulence have been taken. They compared the local time averaged liquid velocity and gas holdup profiles along the radial position.
- Schallenberg et al. (2005) have used 3-D, multi-fluid Eulerian approach for three-phase bubble column. Gas-liquid drag coefficient based on single bubble rise modified for the effect of solid phase. Extended $k-\epsilon$ turbulence model to account for bubble-induced turbulence has been used and the interphase momentum between two dispersed phases included. Local gas and solid holdup as well as liquid velocities have been validated with experimental data.
- Zhang and Ahmadi (2005) have used 2-D, Eulerian-Lagrangian model for three-phase slurry reactor where interactions between bubble-liquid and particle-liquid have been included. Particle-particle and bubble-bubble interactions have been accounted for by the hard sphere model approach. Bubble coalescence has also been included in the model. Transient characteristics of gas, liquid and particle phase flows in terms of flowstructure, effect of bubble size on variation of flow patterns and instantaneous velocities have been studied.

- Panneerselvam et al. (2009) have worked in 3D, Eulerian multi-fluid approach for gas-liquid-solid fluidized bed. Kinetic theory granular flow (KTGF) model for describing the particulate phase and a $k-\epsilon$ based turbulence model for liquid phase turbulence have been used. The interphase momentum between two dispersed phases has been included. Radial distributions of axial and radial solid velocities, axial and radial solid turbulent velocities, shear stress, axial bubble velocity, axial liquid velocity and averaged gas holdup and various energy flows have been studied.
- O'Rourke et al. (2009) have used 3D, Eulerian finite difference approach for gas-liquid-solid fluidized bed. The mathematical model using multiphase particle-in-cell (MP-PIC) method has been used for calculating particle dynamics (collisional exchange) in the Computational-particle fluid dynamics (CPFD). Mass averaged velocity of solid and liquid, particle velocity fluctuation, collision time, and liquid droplet distribution have been studied.
- Jena (2009) has used 2D, Eulerian-Eulerian granular multi-phase approach for gas-liquid-solid fluidized bed. The validation of the proposed CFD model is done with the experimental data for the solid phase, the liquid phase and for the gas phase hydrodynamics. The hydrodynamic parameters studied are bed pressure drop, bed expansion (bed voidage) and gas holdup.
- Chalermssinsuwan et al. (2011). Two- and three-dimensional CFD modeling of Geldart A particles in a thin bubbling fluidized bed. The mathematical model based upon the kinetic theory of granular flow with a modified interphase exchange coefficient was successfully used to compute the system hydrodynamics of fluid catalytic cracking (FCC) particles in a thin bubbling fluidized bed with 2-D and three-dimensional (3-D) computational Domains. Comparison of turbulence and dispersion coefficients of gas.
- Nguyen et al. (2011). have worked in 2-D with Eulerian-Eulerian method for CFD modelling of glass bead particles in a three-phase fluidized bed. The drag model used for simulating is Gidaspow model.
- Kumar et al. (2011). Euler-Euler two-phase fluid model has been used to simulate two-phase (air and water) transient up-flow in bubble column (15cm diameter). The turbulence in the liquid phase is described using the standard $k-\epsilon$ model. Pseudo two phase simulations have been used to model the three phase flow with low solid loadings.

CHAPTER 3

3.0 CFD Modeling of Three Phase Fluidized Bed

3.1 CFD (Computational Fluid Dynamics)

Computational Fluid Dynamics (CFD) is a computer based study-mathematical, computer made related to the dynamics of everything that flows. CFD is one of the branches of Modeling and Simulation, which can imitate a real situation by assuming a mathematical model. For this, it can be considered basic equations, boundary conditions, and constitutive equations. It uses numerical methods to solve the fundamental nonlinear differential equations that describe fluid flow (the Navier-Stokes and allied equations) for predefined geometries and boundary conditions. It is the science of predicting fluid flow, heat transfer, mass transfer, chemical reactions, and related phenomena by solving the mathematical equations which govern these processes using a numerical process.

3.2 Advantages of CFD

- **CFD Saves Cost and Time:** CFD is a very compelling, non-intrusive, virtual modeling technique with powerful visualization capabilities. CFD costs much less than experiments because physical modifications are not necessary.
- **CFD is Reliable:** The numerical schemes and methods upon which CFD is based are improving rapidly, so CFD results are increasingly reliable. CFD is a dependable tool for design and analyses.
- **Speed:** CFD simulations can be executed in a short period of time.
- **Ability to simulate real conditions:** Many flow and heat transfer processes cannot be (easily) tested, e.g. hypersonic flow. CFD provides the ability to theoretically simulate any physical condition.
- **Ability to simulate ideal conditions:** CFD allows great control over the physical process, and provides the ability to isolate specific phenomena for study. Example: a heat transfer process can be idealized with adiabatic, constant heat flux, or constant temperature boundaries.
- **Comprehensive information:** Experiments only permit data to be extracted at a limited number of locations in the system (e.g. pressure and temperature probes, heat flux

gauges, LDV, etc.).CFD allows the analyst to examine a large number of locations in the region of interest, and yields a comprehensive set of flow parameters for examination.

3.3 Limitations of CFD

Physical models:

CFD solutions rely upon physical models of real world processes (e.g. turbulence, compressibility, chemistry, multiphase flow, etc.). The CFD solutions can only be as accurate as the physical models on which they are based.

Numerical errors:

Solving equations on a computer invariably introduces numerical errors.

- Round-off error: due to finite word size available on the computer. Round-off errors will always exist (though they can be small in most cases).
- Truncation error: due to approximations in the numerical models. Truncation errors will go to zero as the grid is refined. Mesh refinement is one way to deal with truncation error.

Boundary conditions:

As with physical models, the accuracy of the CFD solution is only as good as the initial/boundary conditions provided to the numerical model. Example: flow in a duct with sudden expansion. If flow is supplied to domain by a pipe, you should use a fully-developed profile for velocity rather than assume uniform conditions.

3.4 Applications of CFD

Biomedical:

Flow modeling with computational fluid dynamics (CFD) software helps to visualize and predict physical phenomena related to the flow of any substance. It is widely used in medical, pharmaceutical and biomedical applications to analyze:

- manufacturing processes,
- device performance,
- physiological flows,
- fluid-structure interactions,
- The effectiveness of drug delivery systems, etc.

Industrial applications:

CFD is used in wide variety of disciplines and industries, including aerospace, automotive, power generation, chemical manufacturing, polymer processing, petroleum exploration, pulp and paper operation, medical research, meteorology, and astrophysics.

Environmental:

Protecting and improving the quality of our environment today requires innovative design solutions that establish compliance with ever-expanding and more stringent regulations. Flow modeling with Ansys' computational fluid dynamics (CFD) software helps to tackle our environmental flow problems in the most efficient and cost-effective way.

Civil:

Computational Fluid Dynamics (CFD) software is a powerful tool that allows us to create a virtual airflow model of our building or urban environment to assess and optimize these factors before construction commences. Modifications to an existing building can also be simulated using CFD prior to any physical alterations. This approach helps to prevent costly mistakes and minimize design risks while allowing innovation.

3.5 Working of CFD code

In order to provide easy access to their solving power all commercial CFD packages include sophisticated user interfaces input problem parameters and to examine the results. Hence allcodes contain three main elements (Bakker, 2002).

1. Pre-processing
2. Solver
3. Post –processing.

3.5.1 Pre-Processing

In Preprocessing, it consist of input of a flow problem by means of an operator friendly Interface and subsequent transformation of this input into a suitable form which can be used by the solver. This step is performed by software tool such as, GAMBIT, TGRID and DM (Design modular of ANSYS). The Pre-processing stage involves the following steps (Bakker. 2002).

- Defining the geometry of the region for computational domain.
- Generating the Grids for subdivision of the domain into a number of smaller, non-overlapping sub domains.
- Specifying the appropriate boundary and continuum conditions at cells, which coincide with or touch the boundary.

The solution of a flow problem (Phase holdup, velocity, pressure, temperature etc.) is defined in each cell in various nonlinear equations form. The accuracy of CFD solutions is governed by number of cells in the grid. In general, the larger numbers of cells better the solution accuracy.

3.5.2 Solver

The CFD solver does the flow calculations and produces the desired results. ANSYS FLUENT 13 uses the finite-volume method to solve the governing equations for a fluid. It provides the capability to use different physical models such as incompressible or compressible, in viscid or viscous, laminar or turbulent, etc. Governing equations are non-linear and coupled, several iterations of the solution loop are performed by solver before a converged solution is obtained (Bakker., 2002) and the main functions of Solver are as follows:

- Approximation of unknown flow variables by means of simple functions.
- Discretization by substitution of the approximation into the governing flow equations and subsequent mathematical manipulations.
- Solving the algebraic equations.

3.5.3 Post-Processing

This is the final step in CFD analysis, and it involves the results and interpretation of the predicted flow data. ANSYS FLUENT 13 software includes full post processing capabilities and exports CFD data to third-party post-processors and visualization tools such as Ensight, Field view and Tech Plot (Bakker. 2002).

The main outcomes of post processing are -

- Domain geometry & Grid display.
- Contour plot of all the properties.
- Vector plots.
- Animations.
- 2D & 3D surface plots.
- X-Y plots with different properties.
- Particle tracking.
- Plot convergence.
- View manipulation (translation, rotation, scaling etc.)

3.6 Discretization Methods in CFD

There are three discretization methods in CFD:

1. Finite difference method (FDM)
2. Finite volume method (FVM)
3. Finite element method (FEM)

1. Finite difference method (FDM): A finite difference method (FDM) discretization is based upon the differential form of the PDE to be solved. Each derivative is replaced with an approximate difference formula (that can generally be derived from a Taylor series expansion). The computational domain is usually divided into hexahedral cells (the grid), and the solution will be obtained at each nodal point. The FDM is easiest to understand when the physical grid is Cartesian, but through the use of curvilinear transforms the method can be extended to domains that are not easily represented by brick-shaped elements. The discretization results in a system of

equation of the variable at nodal points, and once a solution is found, then we have a discrete representation of the solution.

2. Finite volume method (FVM): A finite volume method (FVM) discretization is based upon an integral form of the PDE to be solved (e.g. conservation of mass, momentum, or energy). The PDE is written in a form which can be solved for a given finite volume (or cell). The computational domain is discretized into finite volumes and then for every volume the governing equations are solved. The resulting system of equations usually involves fluxes of the conserved variable, and thus the calculation of fluxes is very important in FVM. The basic advantage of this method over FDM is it does not require the use of structured grids, and the effort to convert the given mesh in to structured numerical grid internally is completely avoided. As with FDM, the resulting approximate solution is a discrete, but the variables are typically placed at cell centers rather than at nodal points. This is not always true, as there are also face-centered finite volume methods. In any case, the values of field variables at non-storage locations (e.g. vertices) are obtained using interpolation.

3. Finite element method (FEM): A finite element method (FEM) discretization is based upon a piecewise representation of the solution in terms of specified basis functions. The computational domain is divided up into smaller domains (finite elements) and the solution in each element is constructed from the basic functions. The actual equations that are solved are typically obtained by restating the conservation equation in weak form: the field variables are written in terms of the basic functions; the equation is multiplied by appropriate test functions, and then integrated over an element. Since the FEM solution is in terms of specific basis functions, a great deal more is known about the solution than for either FDM or FVM. This can be a double-edged sword, as the choice of basic functions is very important and boundary conditions may be more difficult to formulate. Again, a system of equations is obtained (usually for nodal values) that must be solved to obtain a solution.

Comparison of the three methods is difficult, primarily due to the many variations of all three methods. FVM and FDM provide discrete solutions, while FEM provides a continuous (up to a point) solution. FVM and FDM are generally considered easier to program than FEM, but opinions vary on this point. FVM are generally expected to provide better conservation properties, but opinions vary on this point also.

3.7 Approaches to Multiphase Modeling

For a Multiphase flow there are two approaches for numerical calculations:

1. Euler-Lagrange approach
2. Euler-Euler approach

3.7.1 The Euler Lagrange Approach

This approach is applicable to continuous-dispersed systems and is often referred to as a discrete particle model or particle transport model. The primary phase is continuous and is composed of a gas or a liquid. The secondary phase is discrete and can be composed of particles, drops or bubbles. In the Eulerian-Lagrangian (E-L) approach, the continuous phase is treated in an Eulerian framework (using averaged equations). Its continuous-phase flow field is computed by solving the Navier-Stokes equations. The dispersed phase is represented by tracking a small number of representative particle streams. For each particle stream, ordinary differential equations representing mass, momentum and energy transfer are solved to compute its state and location. The two phases are coupled by inclusion of appropriate interaction terms in the continuous-phase equations. In this approach the volume displaced by the dispersed phase is not taken into account. So, this approach is applicable for low-volume fractions of the dispersed phase. This approach is applicable for situations in which the discrete phase is injected as a continuous stream into the continuous phase. A force balance equation based on Newton's second law of motion is solved to compute the trajectory of the discrete phase. Particle trajectories are computed individually at specified intervals during the fluid phase calculations and dispersed second phase occupies low volume fractions which are the fundamental assumptions in this model.

The Eulerian-Lagrangian approach is suitable to unit operations in which the volume fraction of the dispersed phase is small, such in spray dryers, coal and liquid fuel combustion, and some particle-laden flow. This approach provides complete information on the behavior and residence time of individual particles. Interaction of individual particle streams with turbulent eddies and solid surfaces such as walls can be modeled.

3.7.2 The Euler-Euler Approach

Eulerian-Eulerian approach is the most general approach for solving multiphase flows. It is based on the principle of interpenetrating continua, where each phase is governed by the Navier-Stokes equations. The phases share the same volume and penetrate each other in space and exchange

mass, momentum and energy. Each phase is described by its physical properties and its own velocity, pressure, concentration and temperature field. The interphase transfer between phases is computed using empirical closure relations.

The Eulerian-Eulerian approach is applicable for continuous-dispersed and continuous-continuous systems. For continuous-dispersed systems, the velocity of each phase is computed using the Navier-Stokes equations. The dispersed phase can be in the form of particles, drops or bubbles. The forces acting on the dispersed phase are modeled using empirical correlations and are included as part of the interphase transfer terms. In addition, drag, lift, gravity, buoyancy and virtual-mass effects are some of the forces that might be acting on the dispersed phase. These forces are computed for an individual particle and then scaled by the local volume fraction to account for multiple particles.

In this approach the concept of volume fraction is introduced based upon the fact that the volume of a phase cannot be carried or occupied by other phases. Here the different phases are treated mathematically as interpenetrating continua. The volume fractions are assumed to be continuous functions of space and time and their sum is equal to one. For each of the phase, conservation equations are derived to obtain a set of equations which have similar structure for all phases (Kumar, 2009).

The three different Euler-Euler Multiphase models available are

- The Volume of fluid (VOF) model
- The Mixture Model
- The Eulerian model

1. The VOF Model

In computational fluid dynamics, the Volume of fluid method is one of the most well known methods for volume tracking and locating the free surface. The motion of all phases is modeled by solving a single set of transport equations with appropriate jump boundary conditions at the interface. The VOF model can model two or more immiscible fluids by solving a single set of momentum equations and tracking the volume fraction of each of the fluids throughout the domain. It is generally used to figure out a time dependent solution but for problems which are concerned with steady state solution; it is possible to perform a steady state calculation. A steady state VOF calculation is practical only when the solution is independent of the initial conditions and there are distinct inflow boundaries for the individual phases (Heidari, 2007). Typical

applications include the motion of large bubbles in a liquid, the motion of liquid after a dam break, the prediction of jet breakup, and the steady or transient tracking of any liquid-gas interface. In general, the steady or transient VOF formulation relies on the fact that two or more fluids (or phases) are not interpenetrating.

2. The Mixture Model

The mixture model is a simplified multiphase model that can be used to model multiphase flows where the phases move at different velocities, but assume local equilibrium over short spatial length scales. This model is designed for two or more phases (fluid or particulate). The mixture model can apply to model multiphase flows where the different phases move at different velocities and also it is applicable to model homogeneous multiphase flow and to calculate non-Newtonian viscosity. The mixture model can model n phases (fluid or particulate) by solving both the continuity equation and the momentum equation for the mixture, where mixture can be a combination of continuous phase and the dispersed phase. In addition, the mixture model solves the energy equation for the mixture and the volume fraction equation for the secondary phases, as well as algebraic expressions for the relative velocities (if the phases are moving at different velocities). Also it allows us to select the granular phases and we can calculate the different properties for granular phases. It is applicable in the particle-laden flows with low loading, and bubbly flows where the gas volume fraction remains low, cyclone separators, sedimentation and in liquid-solid flows. It can also be used to model homogenous multiphase flows with very strong coupling and the phases moving at the same velocity. It is a good substitute for the full Eulerian multiphase model in several cases.

3. The Eulerian Model

The Eulerian model is the most complex among other multiphase models. It solves a set of n momentum and continuity equations for each phase coupling is achieved through the pressure and interphase exchange coefficients. The manner of handling of these couplings depends upon the type of phases involved. Granular (fluid-solid) flows are handled differently than non granular (fluid-fluid) flows. For granular flows, the properties are obtained by applying kinetic theory.

3.8 Computational Flow Model

The simulation of three phase fluidized bed is performed by solving the governing equations of mass and momentum conservation using fluent software. Eulerian multi-fluid model is adopted in the present work where gas and liquid phases are all treated as continuous, inter-penetrating and interacting everywhere within the computational domain. The pressure field is assumed to be shared by all the three phases proportional to their volume fraction. Here three dimensional (3D) transient model is developed to simulate the gas hold up of a gas-liquid-solid fluidized bed using the CFD method. The 3D geometry is considered with the quadrilateral-meshing scheme.

Continuity equation:

$$\frac{\delta(\varepsilon_k \rho_k)}{\delta t} + \nabla(\varepsilon_k \rho_k u_k) = 0$$

Where ρ_k is the density and ε_k is the volume fraction of phase $k = \text{gas, liquid, solid}$. The volume fraction of the three phases satisfies the following condition.

$$\varepsilon_L + \varepsilon_s + \varepsilon_g = 1$$

Momentum equations:

For liquid phase

$$\frac{\delta}{\delta t}(\rho_k \varepsilon_k u_k) + \nabla \cdot (\rho_k \varepsilon_k u_k u_k) = -\varepsilon_k \nabla p + \nabla \cdot \tau_k + \rho_k \varepsilon_k g + F_{i,k}$$

Liquid-solid interphase drag force:

The inter-phase exchange coefficient between the liquid and the solid phases, K_{Ls} is obtained by Gidaspow drag model (1994) (it is combination of Wen and Yu model and the Ergun equation) as:

$$K_{Ls} = \frac{150 \cdot \varepsilon_s^2 \cdot \mu_L}{\varepsilon_L d_p^2} + \frac{1.75 \varepsilon_s \rho_L |u_L - u_s|}{\varepsilon_L d_p}, \quad \varepsilon_L \leq 0.8$$

$$K_{Ls} = \frac{3}{4} C_D \varepsilon_s \varepsilon_L \rho_L \frac{(u_L - U_s)}{d_p} f(\varepsilon_L), \quad \varepsilon_L > 0.8$$

Where C_D is the drag co-efficient proposed by wen and yu (1966) and is given as

$$C_D = \frac{24}{\varepsilon_L Re_p} (1 + 0.15 (\varepsilon_L Re_p)^{0.687}) Re_p \leq 1000$$

$$C_D = 0.44 \quad , \quad Re_p \geq 1000$$

Gas-Liquid interphase drag force: The drag model of Schiller and Naumann (1935), acceptable for general use for all fluid-fluid pairs of phases and is given by

$$f = \frac{C_D Re}{24}$$

$$\text{Where } C_D = \frac{24}{Re_p} (1 + 0.15 (Re_b)^{0.687}) , Re_b \leq 1000$$

$$C_D = 0.44 \quad , Re_b \geq 1000$$

3.9 Numerical Methodology

The CFD simulations were carried out for a fluidized bed having diameter 0.1 m and height 1.88 m. The working fluids were water and air. The working solid was spherical glass beads of different diameter. The CFD simulations were performed using commercial CFD code ANSYS FLUENT 13. The assumptions made for hydrodynamic modeling of three phase fluidized bed are Transient as well as unsteady state, Isothermal flow conditions, so no energy equations, Mass transfer and chemical reactions have been neglected, Liquid phase turbulence was modeled using the $k-\varepsilon$ model; the dispersed phases were considered laminar, The system of equations was solved using a finite-volume scheme, Momentum transfer between the liquid and the dispersed phases was modeled using the appropriate drag laws for the respective flow regime, Momentum transfer between the dispersed phases was neglected, Bubbles are assumed as rigid sphere having a constant diameter. The simulation of three phase fluidized bed was performed by solving the governing equations of mass and momentum conservation using fluent software. Eulerian multi-fluid model is adopted in the present work where gas and liquid phases are all treated as continuous, inter-penetrating and interacting everywhere within the computational domain. The pressure field is assumed to be shared by all the three phases proportional to their volume fraction. The motion of each phase is governed by the respective mass and momentum equations. With the Eulerian multiphase model, the number of secondary phases is limited only by memory

requirements and convergence behavior. Any number of secondary phases can be modeled, if sufficient memory is available.

3.9.1 Geometry and Mesh

ANSYS FLUENT 13 is used for making 3D rectangular geometry with width of 0.1m and height 1.88m.

Table 3.1 Mesh Information

| Domain | Node | Element |
|--------|------|---------|
| Fluid | 6095 | 4788 |

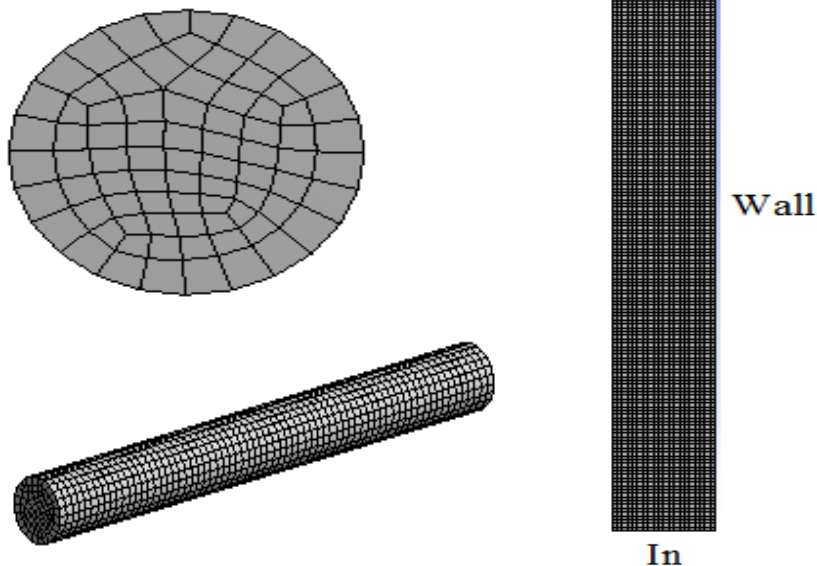


Fig 3.1 3D mesh

3.9.2 Selection of Models for Simulation

ANSYS FLUENT 13.0 is used for simulation. 3D segregated 1st order implicit unsteady solver is used. Standard k- ϵ dispersed Eulerian multiphase model with standard wall functions were used for modeling turbulence. The value of various model constants is tabulated as:

| Model constants | Value |
|-----------------|-------|
| Cmu | 0.09 |
| C1-Epsilon | 1.44 |
| C2-Epsilon | 1.92 |

| | |
|---------------------------|------|
| C3-Epsilon | 1.3 |
| TKE Prandtl Number | 1 |
| TDR Prandtl Number | 1.3 |
| Dispersion Prandtl Number | 0.75 |

Water is taken as continuous phase while glass and air as dispersed phase. Inter-phase interactions formulations used were

- Liquid – Air: Schiller-Naumann
- Solid-Liquid: Gidaspow
- Solid-Air:Gidaspow

Water velocities ranging from 0.2 to 0.16 m/s with increment of 0.02 and air velocities from 0.025 m/s to 0.0875 m/s are used respectively.

3.9.3 Solution

The Phase Coupled SIMPLE method (Patanker, 1980) has been chosen for pressure-velocity coupling. The second-order upwind scheme has been used for discretization of momentum, turbulence kinetic energy and turbulence dissipation rate and the first-order upwind scheme has been used for discretization of volume-fraction equations. The time step size of 0.001s has been used. The convergence criteria for all the numerical simulations are based on monitoring the mass flow residual and the value of $1.0\text{e-}04$ was set as converged value.

The following under relaxation factors have been used for different flow quantities: pressure = 0.5, density = 1, body forces = 1, momentum = 0.2, volume fraction = 0.5, granular temperature = 0.2, turbulent kinetic energy = 0.8, turbulent dissipation rate = 0.8 and turbulent viscosity =1. The simulations have been carried out till the system reached the quasi-steady state i.e., the averaged flow variables are time independent; this can beachieved by monitoring the expanded bed height or phase volume fractions.

RESULT AND DISCUSSION

A gas-liquid-solid fluidized bed of diameter 0.1m and height 1.88 m has been simulated using commercial CFD software package FLUENT 13. Static bed of height 21.3 cm has been used for simulation. Diameter of the glass beads (solid phase) are taken to be 2.18mm. Inlet superficial

velocities of gas are taken in a range of 0.025 m/s to 0.1 m/s while that of water is taken 0.02 m/s to 0.16 m/s. The simulation results obtained have been shown in the figure 3.2.

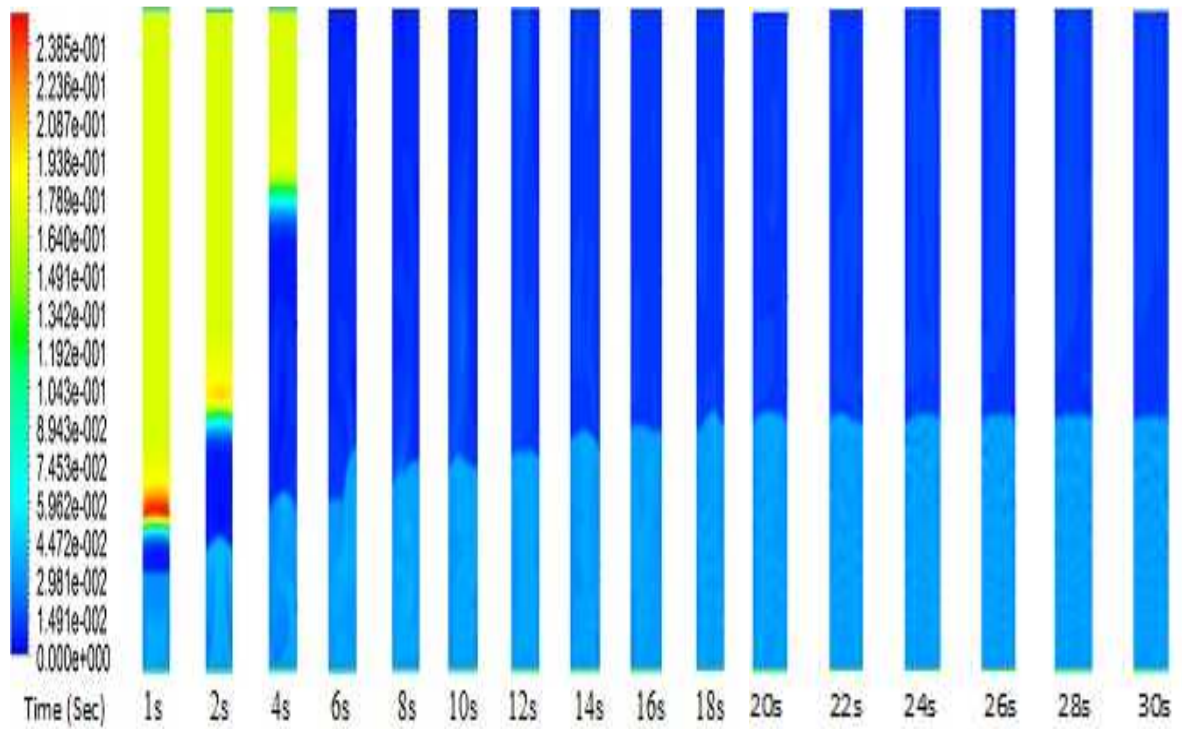


Fig. 3.2 Contours of volume fraction of air at water velocity of 0.12 m/s and air velocity of 0.025 m/s for initial bed height of 21.3 cm.

While simulation takes place, a change in profile is seen in the column, but after some time no significant change is observed which indicates that the quasi steady state has been reached. Simulations are carried out till there is no change in the bed profile. From the figure it is very much clear that the bed profile changes for the first 24 sec, after which there is no subsequent change in the bed profile even though the simulation goes on, like that between 26 to 30 seconds.

3.10 Phase Dynamics

Solid, liquid and gas phase dynamics have been represented in the form of contours. Figure 3.3 shows the contours of volume fraction of solid, liquid and gas in the column obtained at water velocity of 0.12m/s and air velocity of 0.025m/s for static bed height of 21.3 cm after the quasi steady state is achieved. The colour scale given to the left of each contour indicates the value of

volume fraction corresponding to the colour. The contours for glass beads illustrates that bed is in fluidized condition. The contour for water illustrates that volume fraction of the liquid is less in fluidized section than the two-phase region above it. The contour for air illustrates that gas holdup is significantly more in fluidized section of the bed compared to the two-phase region above.

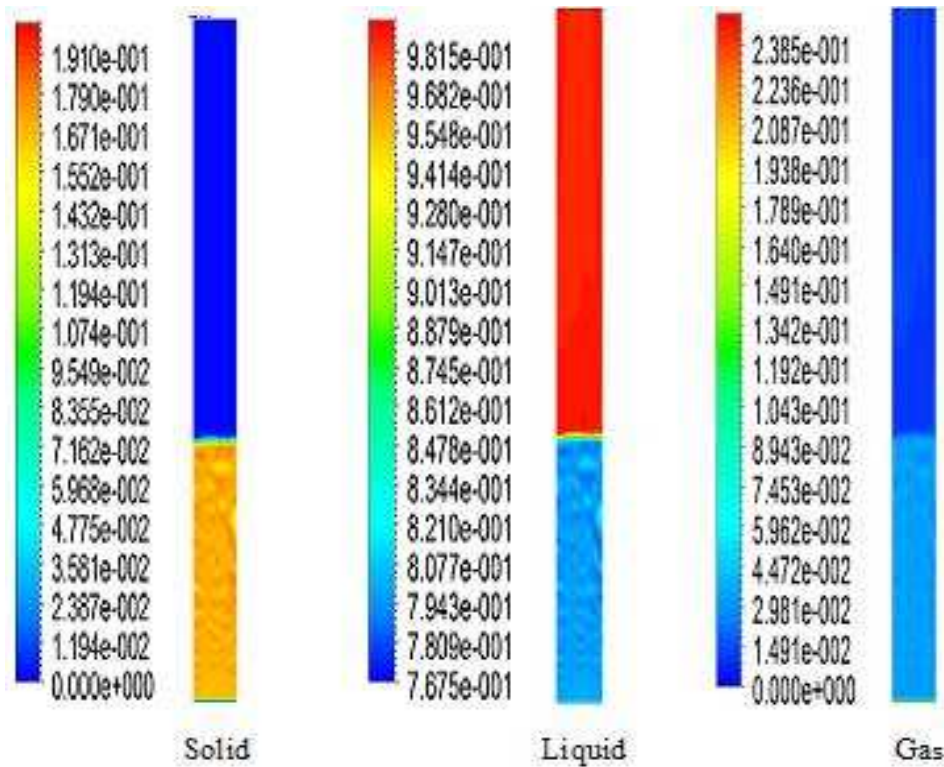


Fig. 3.3 Contours of volume fraction of solid, liquid and gas at water velocity of 0.12 m/s and air velocity of 0.025 m/s for initial static bed height of 0.213 m.

3.11 Gas hold up

The gas holdup values are obtained from CFD simulation. Fig. 3.4 represents the variation of gas holdup in the three-phase fluidized bed with superficial liquid velocity at constant gas velocity for 2.18 mm glass beads at $H_s = 0.213$ m. The gas velocities taken are in the range from 0.025 m/s to 0.1 m/s and the liquid velocities taken are in the range from 0.02 m/s to 0.16 m/s. It is seen from the figure that with increasing liquid velocity, the gas holdup decreases. The decrease in gas holdup with liquid velocity may possibly be due to the fact that at higher liquid velocity

the bubbles are fast driven by the liquid. The residence time of the bubbles decreases with the liquid velocity and hence the gas holdup is likely to decrease.

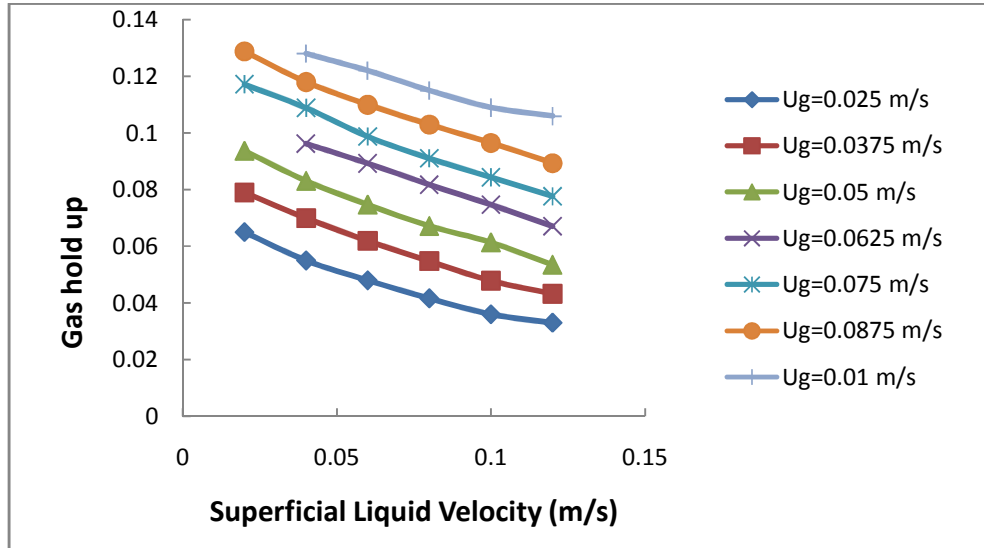


Fig. 3.4 Variation of gas holdup with liquid velocity at constant air velocity for 2.18 mm glass beads at $H_s = 0.213$ m.

The Gas hold up values obtained from experiment, 2D simulation (Jena, 2009) and 3D simulation in present study have been compared here. Fig. 3.5 shows a comparison of the gas holdup values obtained from 3D simulation, 2D simulation and the experimental for air velocity 0.0625 m for initial bed height 21.3 cm.

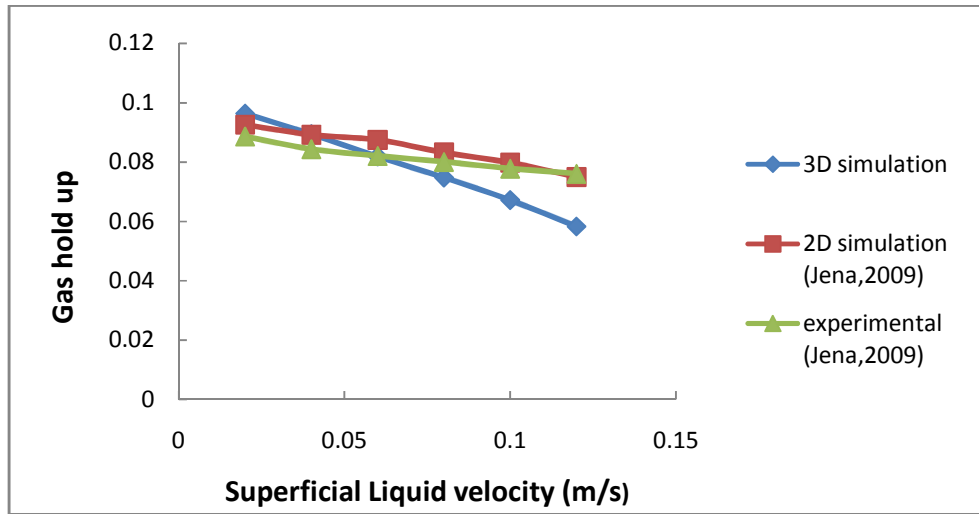


Fig. 3.5 comparison of the gas holdup of air velocity 0.0625 m/s

Fig.3.6 represents the variation of fractional gas holdup with superficial gas velocity, at constant liquid velocity for 2.18 mm glass beads at $H_s=0.213$ m. As seen from the figure, the fractional gas holdup increases monotonically with the gas velocity having little higher value of the slope at low gas velocities. In the lower range of gas velocity, an increase in gas velocity results in the formation of a larger number of gas bubbles without appreciable increase in the bubble diameter. Therefore an increasing fractional gas holdup is observed. As gas velocity increases, the bubble size grows due to bubble coalescence and relatively the gas holdup decreases.

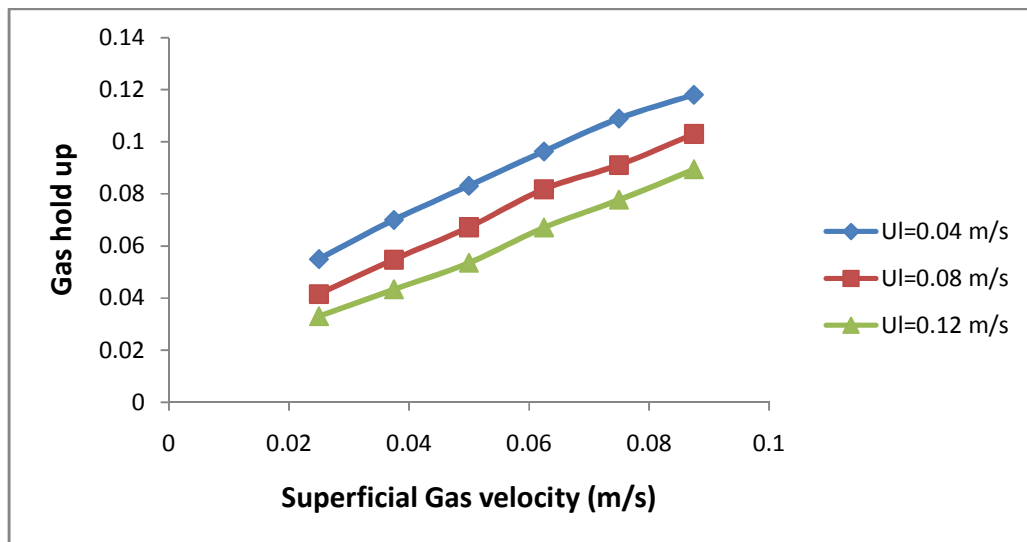


Fig. 3.6 Variation of gas holdup with gas velocity at constant liquid velocity for 2.18 mm glass beads at $H_s= 0.213$ m.

Figure 3.7 shows volume fraction of air along axial direction in 1.88 m fluidized bed at [$V_l=0.12$ m/s, $V_g=0.0375$ m/s, $H_s=0.213$ m, $D_p=2.18$ mm] on x-x' axis. The volume fraction of air is not same at all positions in the fluidized bed, it varies with axial position. Figure shows that initially the liquid volume fraction is constant for some bed height, then it decreases and again it becomes constant along axial direction. The gas holdup is significantly more in fluidized section of the bed compared to the region above.

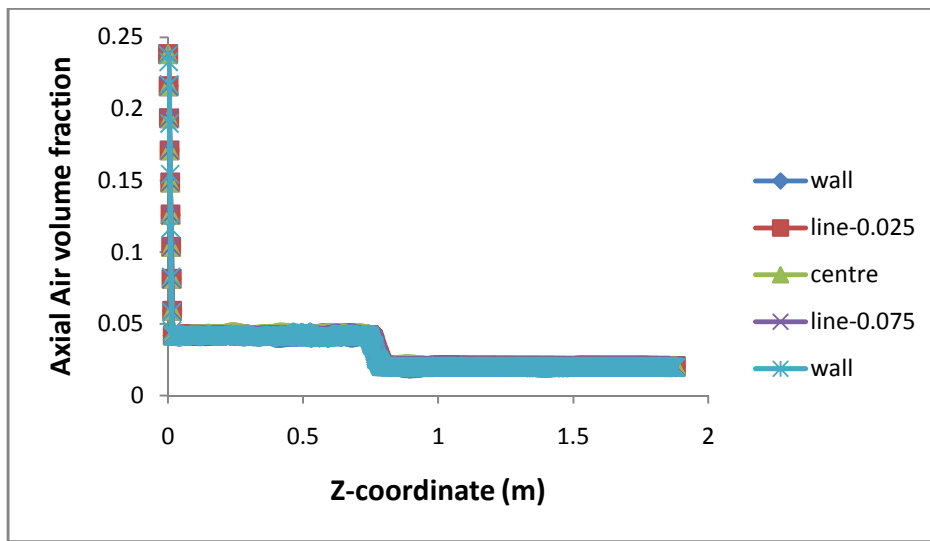


Fig. 3.7 Volume fraction of air along axial direction in 1.88 m fluidized bed at [$V_l=0.12$ m/s, $V_g=0.0375$ m/s, $H_s=0.213$ m, $D_p=2.18$ mm] on x-x' axis

Figure 3.8 shows the volume fraction of solid along axial direction in 1.88 m fluidized bed at water velocity 0.12 m/s and air velocity 0.0375 m/s. In the figure the point where the solid fraction sharply decreases to zero value can be taken as the height of the bed. The volume fraction of the solid is more in fluidized section then it decreases in the above region as no solid particles are present at the top of the column.

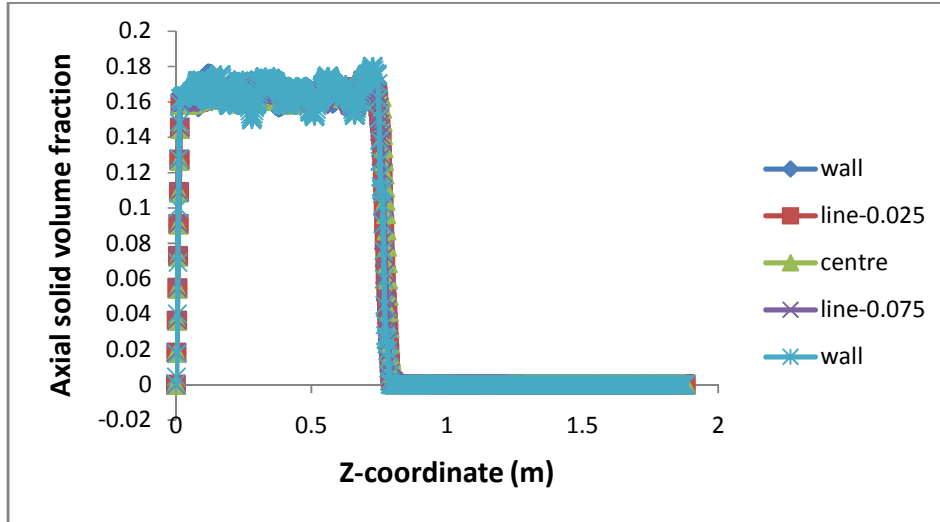


Fig. 3.8 Volume fraction of solid along axial direction in 1.88 m fluidized bed at [$V_l=0.12$ m/s, $V_g=0.0375$ m/s, $H_s=0.213$ m, $D_p=2.18$ mm] on x-x' axis

The volume fraction of liquid along axial direction in 1.88 m fluidized bed is shown in the figure 3.9. It is seen from the figure that initially the liquid volume fraction is constant for some bed height, then it increases and again it becomes constant along axial direction. The volume fraction of the liquid is less in fluidized section than region above.

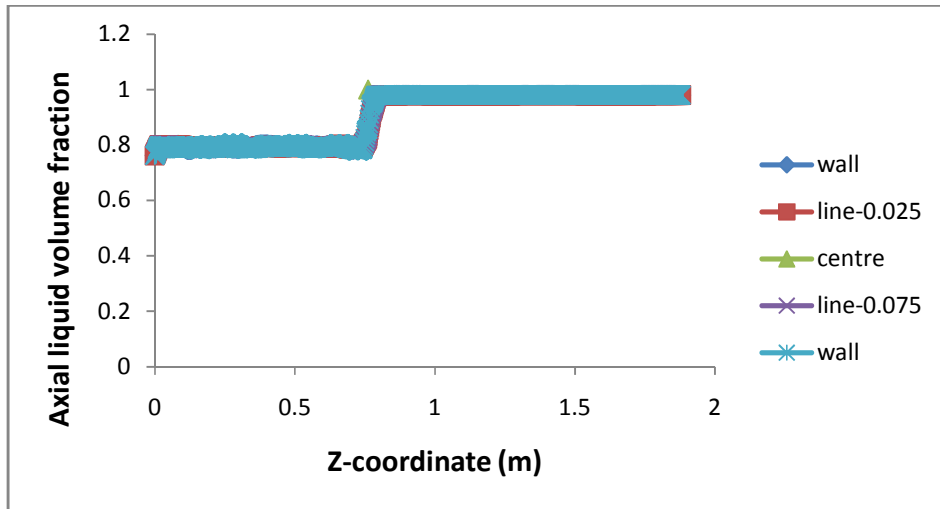


Fig. 3.9 Volume fraction of liquid along axial direction in 1.88 m fluidized bed at [$V_l=0.12$ m/s, $V_g=0.0375$ m/s, $H_s=0.213$ m, $D_p=2.18$ mm] on x-x' axis

The volume fraction of gas, liquid and solid on y-y' axis is similar as on x-x' axis. Figure 3.10 shows the volume fraction of air along axial direction in 1.88 m fluidized bed at $[V_l=0.12 \text{ m/s}, V_g=0.0375 \text{ m/s}, H_s=0.213\text{m}, D_p=2.18\text{mm}]$ on y-y' axis. Figure shows that initially the liquid volume fraction is constant for some bed height, then it decreases and again it becomes constant along axial direction. The gas holdup is significantly more in fluidized section of the bed compared to the region above.

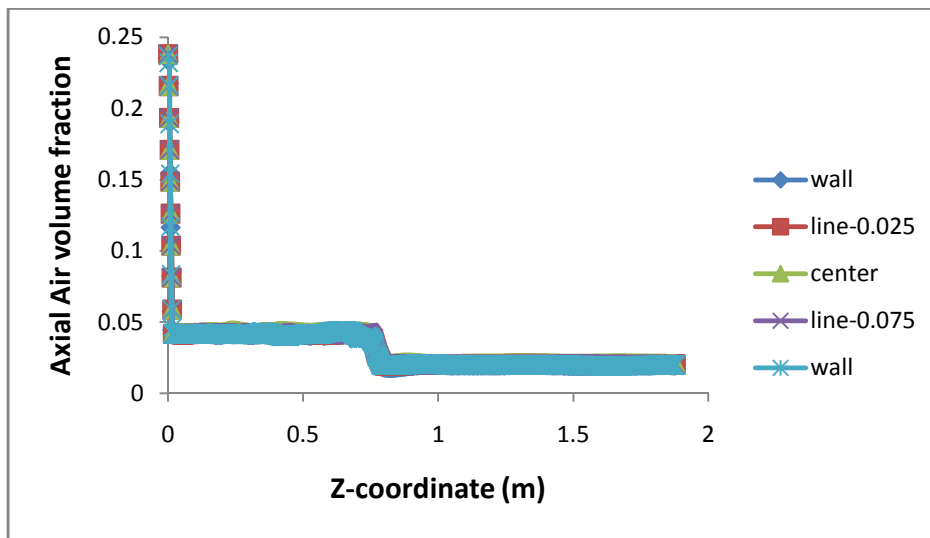


Fig. 3.10 Volume fraction of air along axial direction in 1.88 m fluidized bed at $[V_l=0.12 \text{ m/s}, V_g=0.0375 \text{ m/s}, H_s=0.213\text{m}, D_p=2.18\text{mm}]$ on y-y' axis

Figure 3.11 shows the volume fraction of solid along axial direction in 1.88 m fluidized bed at water velocity 0.12 m/s and air velocity 0.0375 m/s. In the figure the point where the solid fraction sharply decreases to zero value can be taken as the height of the bed. The volume fraction of the solid is more in fluidized section then it decreases in the above region as no solid particles are present at the top of the column.

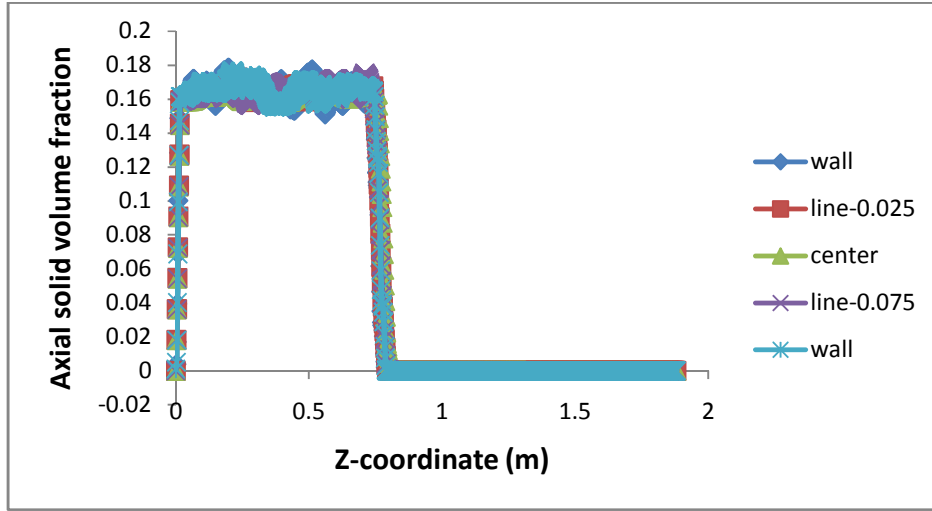


Fig. 3.11 Volume fraction of solid along axial direction in 1.88 m fluidized bed at [$V_I=0.12$ m/s, $V_g=0.0375$ m/s, $H_s=0.213$ m, $D_p=2.18$ mm] on y-y' axis

The volume fraction of liquid along axial direction in 1.88 m fluidized bed is shown in the figure 3.12. It is seen from the figure that initially the liquid volume fraction is constant for some bed height, then it increases and again it becomes constant along axial direction. The volume fraction of the liquid is less in fluidized section than region above.

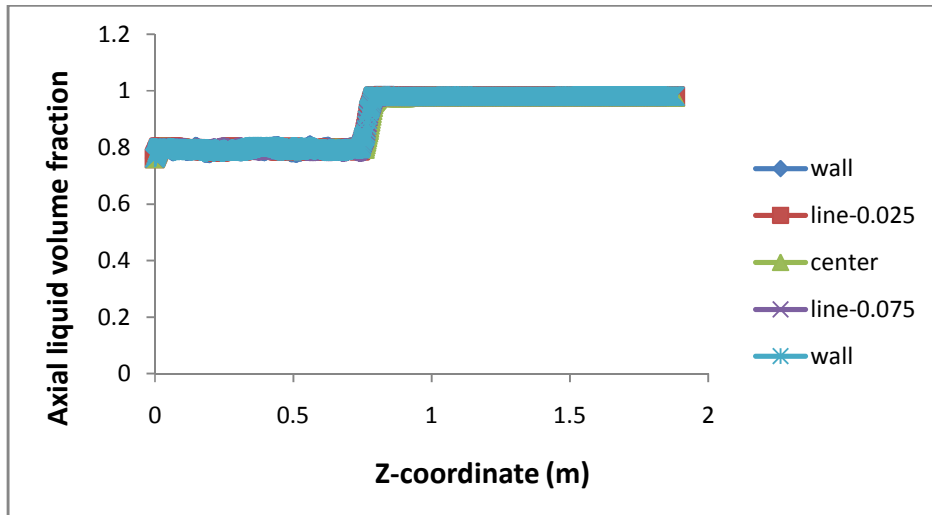


Fig. 3.12 Volume fraction of liquid along axial direction in 1.88 m fluidized bed at [$V_I=0.12$ m/s, $V_g=0.0375$ m/s, $H_s=0.213$ m, $D_p=2.18$ mm] on y-y' axis

The volume fraction of glass bead shows the variation in volume fraction of glass bead along radial direction at different bed heights on x-x' axis. Figure 3.13 shows volume fraction of air with different bed height along radial direction in 1.88 m fluidized bed at [$V_l=0.12$ m/s, $V_g=0.0375$ m/s, $H_s=0.213$ m, $D_p=2.18$ mm]. It is seen from the figure that there is no subsequent change in the volume fraction of air along radial direction. The maximum value of air volume fraction is nearly 0.043 between bed heights 0.1 to 0.6 m. With further increase in bed height there is a decrease in air volume fraction between 0.8 to 1.8 m the air volume fraction is 0.022.

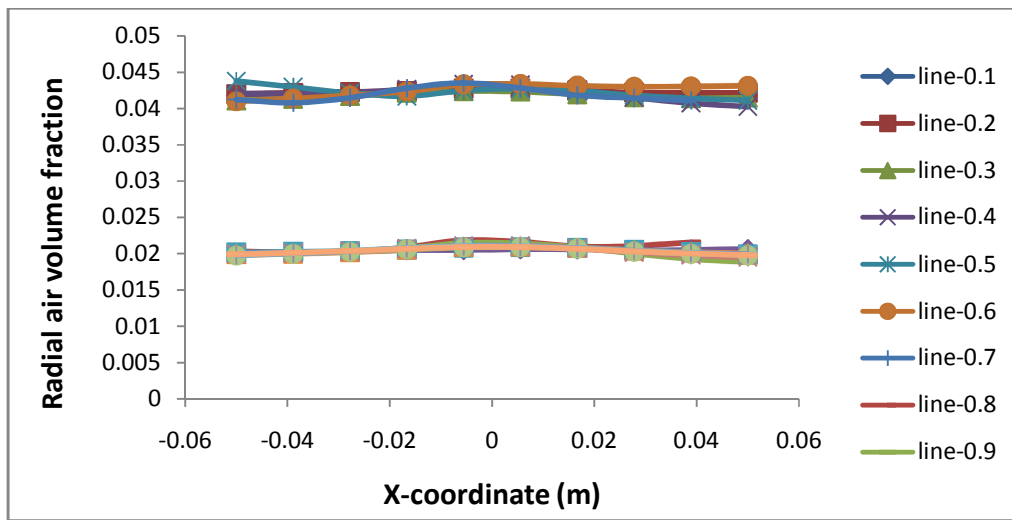


Fig. 3.13 Volume fraction of air with different bed height along radial direction in 1.88 m fluidized bed at [$V_l=0.12$ m/s, $V_g=0.0375$ m/s, $H_s=0.213$ m, $D_p=2.18$ mm] on x-x' axis

Volume fraction of glass bead with different bed height along radial direction in 1.88 m fluidized bed for air velocity of 0.0375 m/s and water velocity 0.12 m/s is shown in figure 3.14. It is seen from the figure that there is no variation in solid volume fraction along the radius. This is because the solid particles are uniformly distributed in the flow field with in the column. The maximum value of air volume fraction is nearly 0.166 between bed heights 0.1 to 0.6 m. With further increase in bed height volume fraction of glass bead decreases and finally reduces to zero since no solid particles are there at the top of the column.

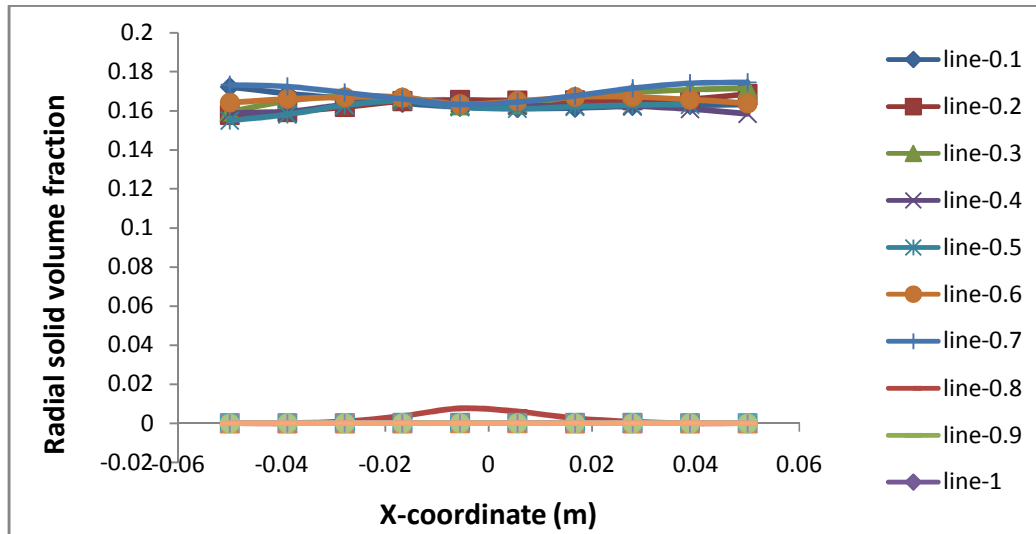


Fig. 3.14 Volume fraction of solid with different bed height along radial direction in 1.88 m fluidized bed at $[V_l=0.12 \text{ m/s}, V_g=0.0375 \text{ m/s}, H_s=0.213\text{m}, D_p=2.18\text{mm}]$ on x-x' axis

Figure 3.15 shows that there is no variation in volume fraction of liquid along the radius. The maximum value of liquid volume fraction is 1 between bed heights 0.8 to 1.8 m. The liquid volume fraction between 0.1 to 0.7 m is 0.8.

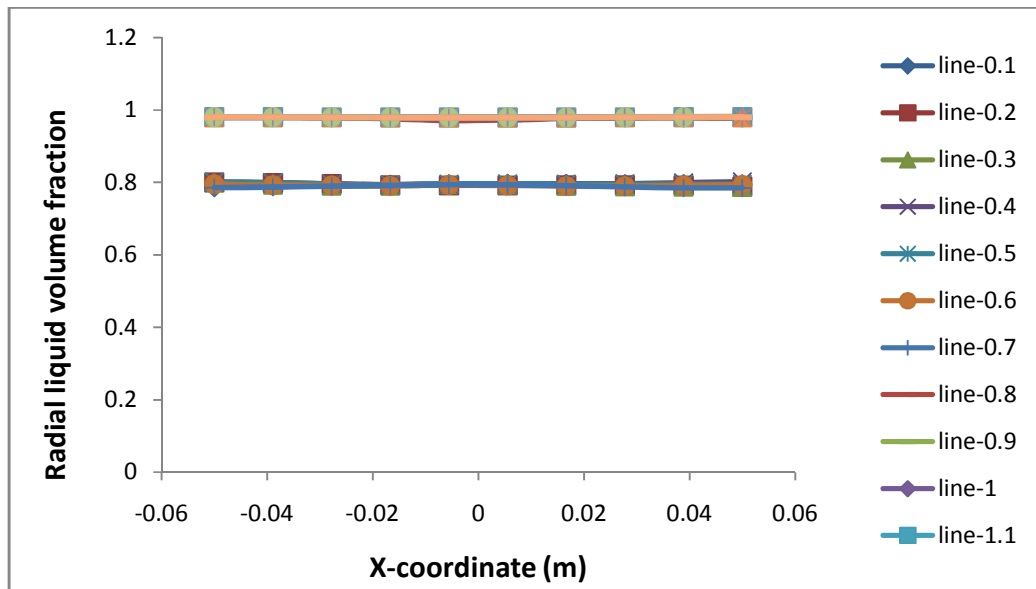


Fig. 3.15 Volume fraction of water with different bed height along radial direction in 1.88 m fluidized bed at $[V_l=0.12 \text{ m/s}, V_g=0.0375 \text{ m/s}, H_s=0.213\text{m}, D_p=2.18\text{mm}]$ on x-x' axis

The magnitude of volume fraction of gas, liquid and solid on y-y' axis are similar as on x-x' axis. Figure 3.16 shows volume fraction of air with different bed height along radial direction in 1.88 m fluidized bed at $[V_l=0.12 \text{ m/s}, V_g=0.0375 \text{ m/s}, H_s=0.213\text{m}, D_p=2.18\text{mm}]$. It is seen from the figure that there is no subsequent change in the volume fraction of air along radial direction. The maximum value of air volume fraction is nearly 0.043 between bed heights 0.1 to 0.6 m. With further increase in bed height there is a decrease in air volume fraction between 0.8 to 1.8 m the air volume fraction is 0.022.

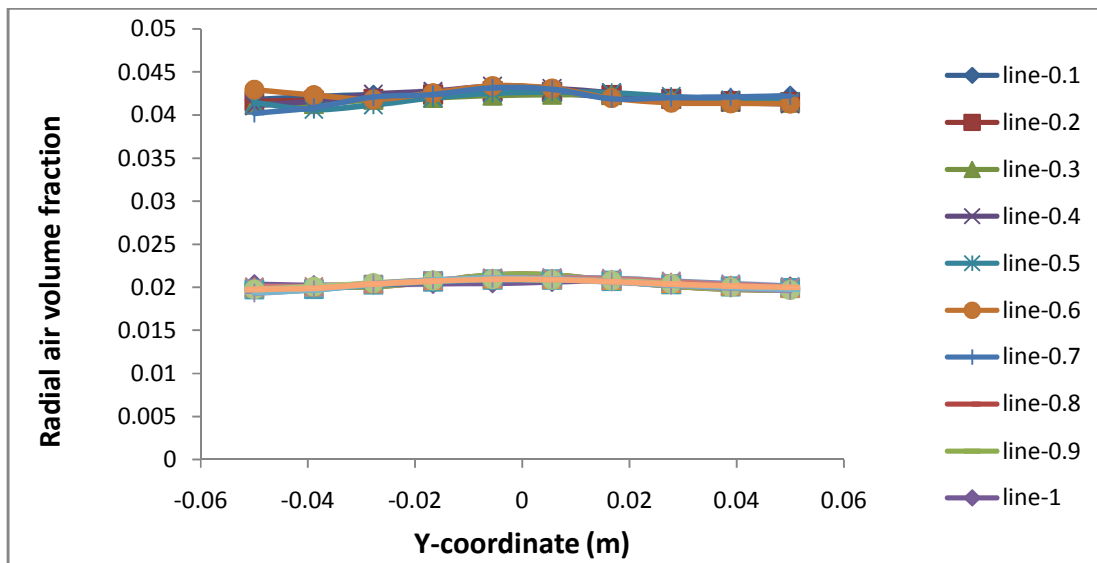


Fig. 3.16 Volume fraction of air with different bed height along radial direction in 1.88 m fluidized bed at $[V_l=0.12 \text{ m/s}, V_g=0.0375 \text{ m/s}, H_s=0.213\text{m}, D_p=2.18\text{mm}]$ on y-y' axis

Volume fraction of glass bead with different bed height along radial direction in 1.88 m fluidized bed for air velocity of 0.0375 m/s and water velocity 0.12 m/s is shown in figure 3.17. It is seen from the figure that there is no variation in solid volume fraction along the radius as solid particles are uniformly distributed in the flow field with in the column. The maximum value of air volume fraction is nearly 0.165 between bed heights 0.1 to 0.6 m. With further increase in bed height volume fraction of glass bead decreases and finally reduces to zero since no solid particles are there at the top of the column.

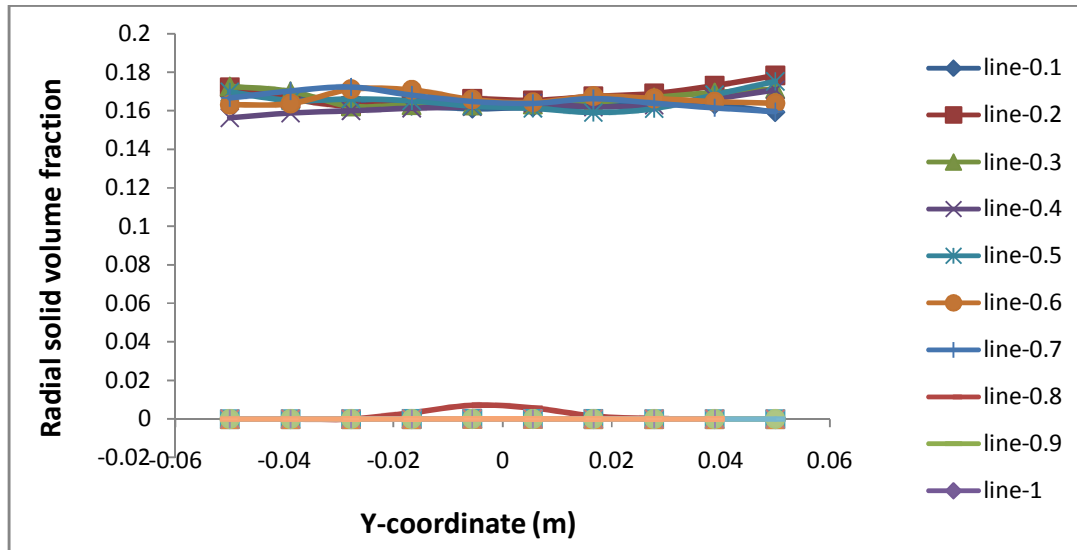


Fig. 3.17 Volume fraction of glass bead with different bed height along radial direction in 1.88 m fluidized bed at [$V_l=0.12$ m/s, $V_g=0.0375$ m/s, $H_s=0.213$ m, $D_p=2.18$ mm] on y-y' axis

Figure 3.18 shows that there is no variation in volume fraction of liquid along the radius. The maximum value of liquid volume fraction is 0.98 between bed heights 0.8 to 1.8 m. The liquid volume fraction between 0.1 to 0.7 m is 0.8.

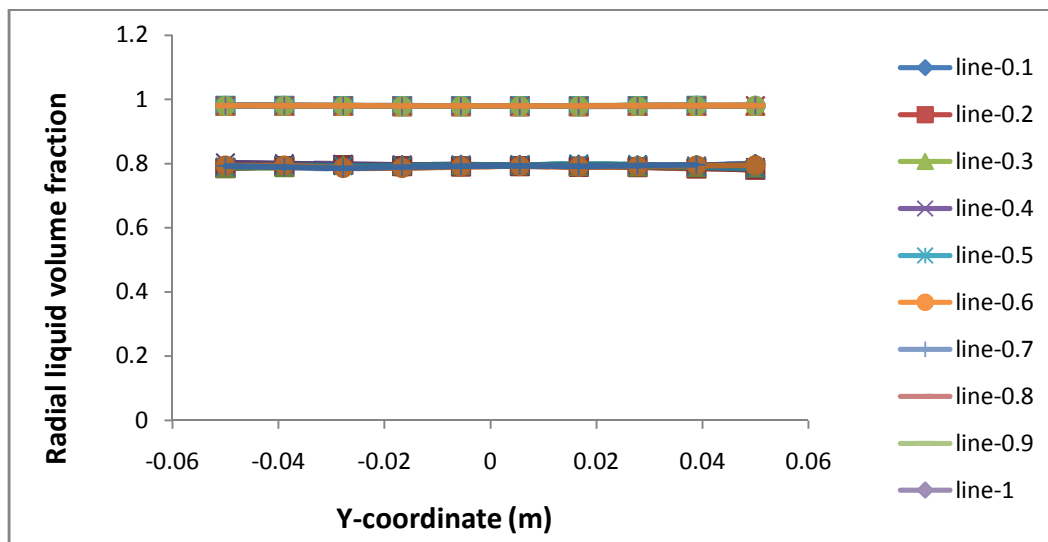


Fig. 3.18 Volume fraction of water with different bed height along radial direction in 1.88 m fluidized bed at [$V_l=0.12$ m/s, $V_g=0.0375$ m/s, $H_s=0.213$ m, $D_p=2.18$ mm] on y-y' axis

3.12 Bed Expansion

In gas-liquid-solid system with increase in liquid velocity at a constant gas velocity, the expanded bed height increases. CFD simulation result also shows an increase in bed expansion with liquid velocity at a constant gas velocity. At low liquid velocity, the bed height has been found to be higher, then it decreases and further increases with increase in liquid velocity.

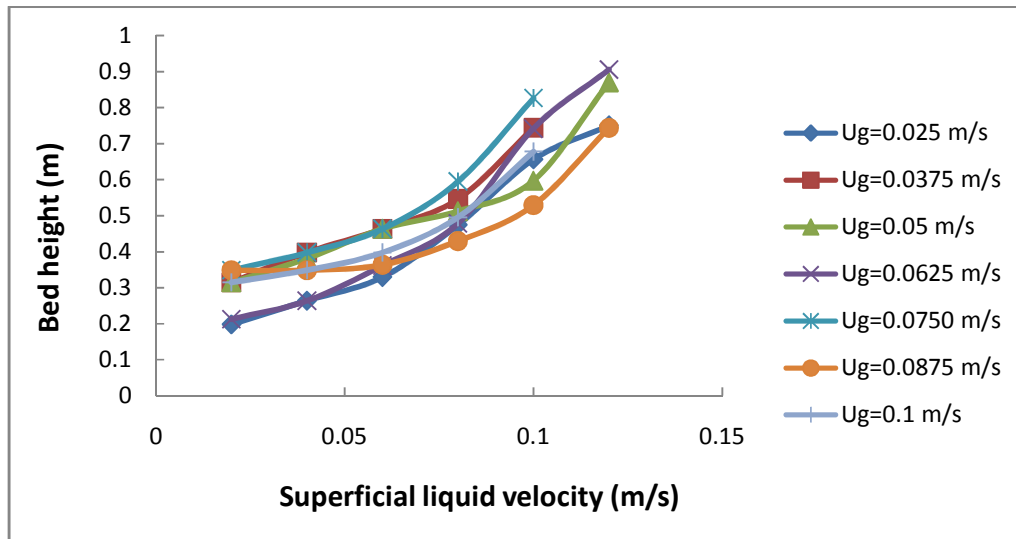


Fig. 3.19 Variation of bed height with liquid velocity for 2.18 mm glass beads at $H_s = 0.213$

Fig. 3.20 shows the variation of bed height with gas velocity for 2.18 mm glass beads at $H_s = 0.213$. It is seen from the figure that with increase in gas velocity at a constant liquid velocity, the expanded bed height has been found to be lower, then it increases and further decreases with increase in gas velocity.

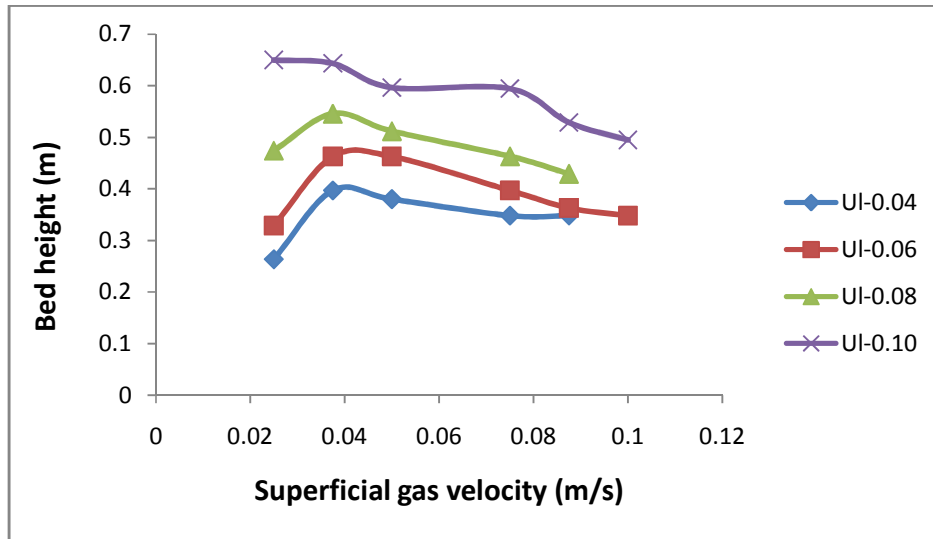


Fig. 3.20 Variation of bed height with gas velocity for 2.18 mm glass beads at $H_s = 0.213$

CHAPTER 4

4.0 CONCLUSION

CFD simulation of hydrodynamics of gas-liquid-solid fluidized bed has been carried out for different operating conditions by employing the Eulerian-Eulerian granular multiphase approach. The hydrodynamic parameters studied are gas hold up, bed expansion and operating variables varied are gas and liquid velocity.

Main conclusions that can be drawn are:

- Gas holdup is more in fluidized part of the bed as illustrated by the contours for air.
- Contour of volume fraction of water shows that the volume fraction of water is less in fluidized part of the column in comparison to the rest part.
- Bed expands when liquid velocity is increased at constant air velocity as illustrated from the plot of bed expansion vs liquid velocity.
- With increase in gas velocity at a constant liquid velocity, the expanded bed height initially increases and then decreases.
- Trends of gas holdup vs. inlet air velocity shows that gas holdup increases with increase in air velocity obtained at constant water velocity.
- Trends of gas holdup vs. inlet Water velocity show that gas holdup decreases with the increase in inlet water velocity at constant air velocity.
- Volume fraction of gas, liquid and solid with different bed height along radial direction shows that there is no variation in the volume fractions along the radius.

REFERENCES

- Bahary, M., 1994. Experimental and computational studies of hydrodynamics in three-phase and two-phase fluidized beds. Ph.D. Thesis, Illinois Institute of Technology, Chicago.
- Bhatia, V.K., Epstein, N. 1974. Three Phase Fluidization: A Generalized Wake Model. In: Fluidization and its Applications. H. Angelino et al., Eds., Cepadues Editions, Toulouse, 380-392.
- Briens, L.A., Ellis, N., 2005. Hydrodynamics of three-phase fluidized bed systems examined by statistical, fractal, chaos and wavelet analysis methods. Chemical Engineering Science 60, 6094-6106.
- Chen, Z., Zheng, C., Feng, Y., 1995. Distributions of flow regimes and phase holdups in three-phase fluidised beds. Chemical Engineering Science 50, 2153-2159.
- Chalermsoinsuwan, B., Gidaspow, D., Piumsomboon, P., 2011. Two and three-dimensional CFD modeling of Geldart A particles in a thin bubbling fluidised bed: Comparison of turbulence and dispersion coefficients. Chemical Engineering Journal 171, 301-313.
- Epstein, N., 1981. Review: Three-Phase Fluidization-Some Knowledge Gaps. Canadian Journal of Chemical Engineering 59, 649-757.
- Fan, L.S., 1989. Gas-Liquid-Solid Fluidization Engineering. Butterworth Series in Chemical Engineering, Butterworth Publishers, Boston, MA.
- Fraguío, M.S., Cassanello, M.C., Larachi, F., Chaouki, J., 2006. Flow regime transition pointers in three-phase fluidised beds inferred from a solid tracer trajectory. Chemical Engineering and Processing 45, 350-358.
- Feng, W., Wen, J., Fan, J., Yuan, Q., Jia, X., Sun, Y., 2005. Local hydrodynamics of gas-liquid-nano particles three-phase fluidization. Chemical Engineering Science 60, 6887-6898.
- Grevschott, S., Sannaes, B.H., Dudukovic, M.P., Hjarbo, K.W., Svendsen, H.F., 1996. Liquid circulation, bubble size distributions, and solids movement in two-and three-phase bubble columns. Chemical Engineering Science 51, 1703-1713.

- Jena, H.M., Sahoo, B.K., Roy, G.K., Meikap, B.C., 2008. Characterization of hydrodynamic properties of a gas–liquid–solid three-phase fluidized bed with regular shape spherical glass bead particles. *Chemical Engineering Journal* 145, 50-56.
- Jena H.M, 2009. Hydrodynamics of Gas-Liquid-Solid Fluidized and Semi-Fluidized Beds. Ph.D. Thesis, National Institute of Technology, Rourkela.
- Jianping, W., Shonglin, X., 1998. Local hydrodynamics in a gas-liquid-solid three-phase bubble column reactor. *Chemical Engineering Journal* 70, 81-84.
- Kiared, K., Larachi, F., Chaouki, J., Guy, C., 1999. Mean and turbulent particle velocity in the fully developed region of a three-phase fluidised bed. *Chemical Engineering & Technology* 22, 683-689.
- Kumar, S., Srinivasulu, N., Khanna, A., 2011. CFD Simulations to Validate Two & Three Phase Up-flow in Bubble Columns. *World Academy of Science, Engineering and Technology* 59,2223-2228.
- Lee, S.L.P., de Lasa, H.I., 1987. Phase holdups in three-phase fluidized beds. *AIChE Journal* 33, 1359-1370.
- Li, Y., Zhang, J., Fan, L.S., 1999. Numerical simulation of gas-liquid-solid fluidization systems using a combined CFD-VOF-DPM method: bubble wake behavior. *Chemical Engineering Science* 54, 5101-5107.
- Matonis, D., Gidaspow, D., Bahary, M., 2002. CFD simulation of flow and turbulence in a slurry bubble column. *AIChE Journal* 48, 1413–1429.
- Mitra-Majumdar, D., Farouk, B., Shah, Y.T., 1997. Hydrodynamic modeling of three-phase flows through a vertical column. *Chemical Engineering Science* 52, 4485-4497.
- Muroyama, A., Fan, L.S., 1985. Fundamentals of gas–liquid–solid fluidization. *A.I.Ch.E. Journal* 30, 1-34.
- Nguyen, K.T., Huang, S., 2011. Simulation of Hydrodynamic Characteristics of Glass Beads in Gas-Liquid-Solid Three Phase Fluidized Beds by Computational Fluid Dynamics. *Journal of Engineering Technology and Education* 8, 248-261.
- O'Rourke, P.J., Zhao, P.(P.), Snider, D., 2009. A model for collisional exchange in gas/liquid/solid fluidized beds. *Chemical Engineering Science* 64, 1784-1797.

- Padial, N.T., Van der Heyden, W.B., Rauenzahn, R.M., Yarbro, S.L., 2000. Three dimensional simulation of a three-phase draft-tube bubble column. *Chemical Engineering Science* 55, 3261-3273.
- Panneerselvam, R., Savithri, S., Surender, G.D., 2009. CFD simulation of hydrodynamics of gas–liquid–solid fluidised bed reactor. *Chemical Engineering Science* 64, 1119-1135.
- Rigby, G.R., Van Brokland, G.P., Park, W.H., Capes, C.E., 1970. Properties of bubbles in three-phase fluidized bed as measured by an electroresistivity probe. *Chemical Engineering Science* 25, 1729–1741.
- Safoniuk, M., Grace, J.R., Hackman, L., Mcknight, C.A., 2002. Gas Hold-Up in a Three-Phase Fluidized Bed. *AIChE Journal* 48, 1581-1587.
- Schallenberg, J., En, J.H., Hempel, D.C., 2005. The important role of local dispersed phase hold-ups for the calculation of three-phase bubble columns. *Chemical Engineering Science* 60, 6027–6033.
- Sokol, W., Halfani, M.R., 1999. Hydrodynamics of a gas-liquid-solid fluidized bed bioreactor with a low-density biomass support. *Biochemical Engineering Journal* 3, 185-192.
- Warsito, W., Fan, L.S., 2001. Measurement of real-time flow structures in gas-liquid and gas-liquid–solid flow systems using electrical capacitance tomography (ECT). *Chemical Engineering Science* 56, 6455–6462.
- Zhang, X., Ahmadi, G., 2005. Eulerian-Lagrangian simulations of liquid-gas-solid flows in three-phase slurry reactors. *Chemical Engineering Science* 60, 5089-5104.